Torque-Bounded Admittance Control Realized by a Set-Valued Algebraic Feedback

Ryo Kikuuwe, *Member, IEEE*

***Abstract*—This paper proposes a new admittance controller that realizes safe behavior even under torque saturation. The new controller is analytically equivalent to a conventional admittance controller as long as the actuator torque is not saturated, but is free from unsafe behaviors such as snapping back, oscillation, or overshoots, which may happen with conventional admittance controllers after torque saturation. The new controller is described by a differential algebraic inclusion, and can be understood as a conventional admittance controller expanded with an additional algebraic loop through a normal-cone operator. Its continuous-time representation involves a nonsmooth, set-valued function, but its discrete-time implementation is free from set-valuedness and given as a closed-form algorithm as a result of the use of implicit (backward) Euler discretization. The controller is tested with one joint of an industrial manipulator equipped with a force sensor.**

***Index Terms*—Actuator saturation, differential inclusion, force control, normal cone.**

I. Introduction

ADMITTANCE control is a control scheme to regulate the reaction of the robot against the contact force applied to the robot's end-effector. It is one form of impedance control in a broad sense and is also referred to as a "position-based impedance control." Typical implementation of an admittance controller is illustrated in Fig. 1(a). It employs a force sensor mounted on the end-effector, and it consists of a "proxy" (a virtual object) representing a simple dynamics, typically a damped mass element, and a high-gain position controller. The position q_x of the proxy is updated according to the force sensor measurement f and the commanded force f_d. The resultant proxy position q_x is used as the position command to the internal position controller that forces the robot's position q_s to follow q_x. The advantage of this controller structure is that the internal position controller suppresses the hardware dynamics, such as joint friction. Its applications include haptic interfaces [1], [2], manual guidance of industrial manipulators [3], human–robot collaboration [4], robotic orthoses [5], [6], and surgical robots [7].

One problem of this control scheme is that, when the proxy is far separated from the robot position, the behavior of the robot becomes unpredictable. Such situations happen when a large external force is applied to a portion other than the force sensor and the torque[1] exerted by the position controller is saturated. Another complicated situation happens when the robot position is constrained by an external object while another force is applied to the force sensor. In such a situation, the proxy may move away from the robot position, even beyond the motion range of the robot. After these cases happen, once the external force is removed, the robot is attracted to the proxy, causing a snapping-back behavior with overshoots and oscillations. Such behaviors may cause damage to the robot hardware and surrounding objects and also injury to human operators.

In a previous paper [8], Kikuuwe proposed an internal position controller for admittance control to attenuate the undesirable effects of torque saturation. The controller was an extension of a "proxy-based sliding mode control" [9], [10], which has been proposed by Kikuuwe *et al.* Experimental results have shown that the admittance control scheme proposed in [8] is

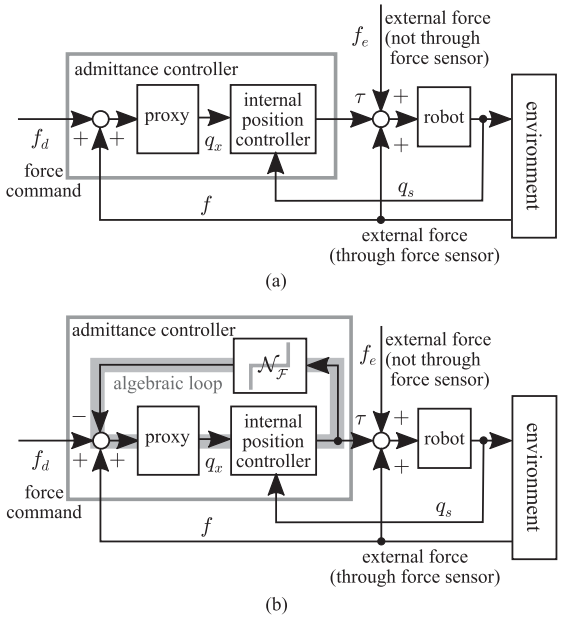

Fig. 1. Systems controlled with admittance controllers. (a) Typical implementation. (b) Proposed implementation.

Manuscript received November 22, 2018; accepted May 23, 2019. Date of publication June 20, 2019; date of current version October 1, 2019. This paper was recommended for publication by Associate Editor P. Fraisse and Editor I.-M. Chen upon evaluation of the reviewers' comments. This work was supported by the Grant-in-Aid for Scientific Research (15H03938) from Japan Society for the Promotion of Science.

The author is with the Hiroshima University, Higashi-Hiroshima 739-8527, Japan (e-mail: kikuuwe@ieee.org).

Color versions of one or more of the figures in this paper are available online at http://ieeexplore.ieee.org.

Digital Object Identifier 10.1109/TRO.2019.2920069

[1] Because this paper mostly deals with one-dimensional (1-D) systems, which can be either translational or rotational, this paper does not strictly distinguish the terminology of translational and rotational systems. Both "external force" and "actuator torque" mean generalized forces in 1-D systems.

effective in cases where short-time saturations frequently happen. It however was not intended for the situation where the torque is saturated for a long time, e.g., where a human user intentionally interrupts the robot's motion by pushing the robot's links.

This paper proposes a new admittance controller that allows torque saturation in a more natural manner. It behaves as an ordinary admittance controller as long as the actuator torque is within the predetermined range, but it yields to the external force without making overshoots or oscillations when the torque is saturated. The proposed technique comprises an algebraic loop, as in Fig. 1(b), which forms an algebraic constraint between the proxy position and the actuator torque. The whole controller is described as a differential algebraic inclusion (DAI) and its discrete-time implementation is derived through the implicit (backward) Euler discretization.

The rest of this paper is organized as follows. Section II provides mathematical preliminaries to deal with set-valued functions and an overview on related work. Section III proposes a new admittance controller and provides stability analysis. Section IV shows results of experiments employing an industrial manipulator. Section V presents some additional modifications and the results of experiments showing the effects of the modifications. Section VI concludes this paper.

II. Preliminaries

A. Mathematical Preliminaries

Let $\mathcal{A}$ be a closed interval of real numbers. This paper uses the following functions:

$$\mathrm{proj}_{\mathcal{A}}(x) \triangleq \operatorname*{argmin}_{\xi\in\mathcal{A}} (\xi - x)^2 \tag{1}$$

$$\mathrm{dzn}_{\mathcal{A}}(x) \triangleq x - \mathrm{proj}_{\mathcal{A}}(x) \tag{2}$$

$$\mathcal{N}_{\mathcal{A}}(x) \triangleq \begin{cases} \{\xi \in \mathcal{R} \,|\, \xi(x^* - x) \le 0 \ \forall x^* \in \mathcal{A}\} & \\ \qquad\qquad\qquad\qquad \text{if } x \in \mathcal{A} & \\ \emptyset \qquad\qquad\qquad\qquad \text{if } x \notin \mathcal{A}. & \end{cases} \tag{3}$$

Here, $\mathrm{proj}_{\mathcal{A}}$ is a projection function onto the set $\mathcal{A}$, $\mathrm{dzn}_{\mathcal{A}}$ is a dead zone function with respect to the set $\mathcal{A}$, and $\mathcal{N}_{\mathcal{A}}(x)$ is the normal cone of the set $\mathcal{A}$ at the point x. If the set $\mathcal{A}$ is written as $\mathcal{A} = [A, B]$ where $A \le B$, these functions can be written as follows:

$$\mathrm{proj}_{[A,B]}(x) = \begin{cases} B & \text{if } x > B \\ x & \text{if } x \in [A, B] \\ A & \text{if } x < A \end{cases} \tag{4}$$

$$\mathrm{dzn}_{[A,B]}(x) = \begin{cases} x - B & \text{if } x > B \\ 0 & \text{if } x \in [A, B] \\ x - A & \text{if } x < A \end{cases} \tag{5}$$

$$\mathcal{N}_{[A,B]}(x) = \begin{cases} \emptyset & \text{if } x > B \ \wedge \ x < A \\ [0, \infty) & \text{if } x = B \neq A \\ 0 & \text{if } x \in (A, B) \\ (-\infty, 0] & \text{if } x = A \neq B \\ (-\infty, \infty) & \text{if } x = A = B \end{cases}. \tag{6}$$

These functions are illustrated in Fig. 2.

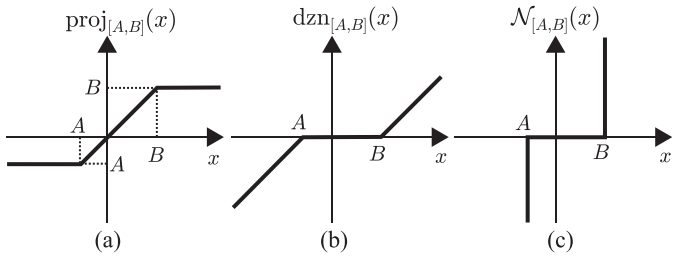

Fig. 2. Functions $\mathrm{proj}_{[A,B]}(x)$, $\mathrm{dzn}_{[A,B]}(x)$, and $\mathcal{N}_{[A,B]}(x)$ with $A < B$.

The following relation exists between the projection and the normal cone [11, Sec. A.3]:

$$x + \mathcal{N}_{\mathcal{A}}(x) \ni y \iff x = \mathrm{proj}_{\mathcal{A}}(y). \tag{7}$$

Here, the addition and subtraction between a set $\mathcal{B}$ and a single value x is understood as

$$\mathcal{B} \pm x = \bigcup_{\eta\in\mathcal{B}} (\eta \pm x). \tag{8}$$

This implies that, if $\mathcal{B} = [A, B]$, $\mathcal{B} + x = [A + x, B + x]$.

This paper also uses the following set-valued signum function:

$$\mathrm{sgn}(x) \triangleq \begin{cases} [-1, 1] & \text{if } x = 0 \\ x/|x| & \text{if } x \neq 0. \end{cases} \tag{9}$$

With a nonnegative scalar $F \ge 0$, the normal cone of a symmetric closed interval $[-F, F]$ can be seen as the inverse map of the signum function as follows:

$$x \in F\mathrm{sgn}(y) \iff \mathcal{N}_{[-F,F]}(x) \ni y. \tag{10}$$

The relation between the signum function and the saturation function can be written as follows:

$$x \in F\mathrm{sgn}(y - x) \iff x = \mathrm{proj}_{[-F,F]}(y), \tag{11}$$

which is a special case of (7).

This paper also uses the notation $\mathrm{co}(\mathcal{X})$ to denote the convex hull of the set $\mathcal{X}$. With two scalars A and B, $\mathrm{co}(\{A, B\}) = \mathrm{co}(\{B, A\}) = [\min(A, B), \max(A, B)]$. With two sets $\mathcal{A}$ and $\mathcal{B}$, the addition and the subtraction are defined as

$$\mathcal{A} \pm \mathcal{B} = \bigcup_{\xi\in\mathcal{A}} \bigcup_{\eta\in\mathcal{B}} (\xi \pm \eta) \tag{12}$$

respectively. The following fact should be noted:

$$\begin{aligned} \mathcal{A} - \mathcal{B} \ni 0 &\iff \exists \eta \in \mathcal{B} \text{ s.t. } \mathcal{A} - \eta \ni 0 \\ &\iff \mathcal{A} \cap \mathcal{B} \neq \emptyset. \end{aligned} \tag{13}$$

In addition, with two set-valued functions[2] $\Phi : \mathbb{R} \rightrightarrows \mathbb{R}$ and $\Psi : \mathbb{R} \rightrightarrows \mathbb{R}$, the nested expression $\Psi(\Phi(x) + y)$ should be understood as follows:

$$\Psi(\Phi(x) + y) = \bigcup_{\eta\in\Phi(x)} \Psi(\eta + y). \tag{14}$$

[2] The notation $\Phi : \mathbb{R} \rightrightarrows \mathbb{R}$ means that Φ is a set-valued function, as opposed to a single-valued function, which is often declared as $\Phi : \mathbb{R} \to \mathbb{R}$.

B. Conventional Admittance Controller

Let us consider a 1-D system composed of a single mass, which is hereafter referred to as the controlled object. Let $q_s \in \mathbb{R}$ be the measured position of the controlled object, $\tau \in \mathbb{R}$ be the actuator force, and $f \in \mathbb{R}$ be the force measured through the force sensor and applied to the controlled object. In addition, let $f_d \in \mathbb{R}$ be a force command provided by an upper level controller or the user. The task here is to realize desired inertia $M_x > 0$ and viscosity $B_x > 0$ in the relation between the position q_s and the force $f + f_d$, i.e., to realize the relation $\mathcal{L}[q_s] \approx \mathcal{L}[f + f_d]/(M_x s^2 + B_x s)$. We consider the following typical and conventional admittance controller:

$$M_x \ddot{q}_x + B_x \dot{q}_x = f + f_d \tag{15a}$$

$$\dot{a} = q_x - q_s \tag{15b}$$

$$\tau = M\ddot{q}_x + K(q_x - q_s) + B(\dot{q}_x - \dot{q}_s) + La. \tag{15c}$$

Here, $q_x \in \mathbb{R}$ is the position of the proxy, which has the designed dynamics represented by (15a). The lines (15b) and (15c) represent a proportional-derivative-integral (PID) position controller with a feedforward of the desired acceleration. The coefficients K, B, and L are proportional, derivative, and integral gains, respectively, which should be set as high as permitted by the stability of the closed-loop system. The coefficient M is a positive constant, which should be chosen to be close to the inertia of the controlled object. When the robot is statically in contact with an environment surface, f_d can be interpreted as the desired value of $-f$. In such a situation, the quantity $f + f_d$ can be seen as the error in the contact force. The controller (15) is illustrated in Fig. 1(a).

Here, we discuss stability and convergence properties of the conventional admittance controller (15). Let us consider that the controller (15) is applied to the following simple plant:

$$M_r \ddot{q}_s + B_r \dot{q}_s = \tau + f + f_e. \tag{16}$$

This plant is a single mass $M_r > 0$ of which the position is q_s and is subjected to an external disturbance f_e. The force f applied to the force sensor is used in the controller (15) and also affects the plant directly as in the right-hand side of (16). From (15) and (16), one has the following relation:

$$\mathcal{L}[q_s] = \frac{U_1(s)\mathcal{L}[f] + U_2(s)\mathcal{L}[f_d]}{M_x s^2 + B_x s} + E_1(s)\mathcal{L}[f_e] \tag{17}$$

where $\mathcal{L}$ denotes the Laplace transform, s is the Laplace operator, and

$$U_1(s) \triangleq \frac{(M + M_x)s^3 + (B + B_x)s^2 + Ks + L}{M_r s^3 + (B + B_r)s^2 + Ks + L} \tag{18}$$

$$U_2(s) \triangleq \frac{Ms^3 + Bs^2 + Ks + L}{M_r s^3 + (B + B_r)s^2 + Ks + L} \tag{19}$$

$$E_1(s) \triangleq \frac{s}{M_r s^3 + (B + B_r)s^2 + Ks + L}. \tag{20}$$

From the Routh-Hurwitz stability criterion, one can see that the system is stable only if $K(B + B_r) > LM_r$. If this inequality is satisfied and $U_1(s) \approx 1$, $U_2(s) \approx 1$, and $E_1(s) \approx 0$ are also satisfied, we have $\mathcal{L}[q_s] \approx \mathcal{L}[f + f_d]/(M_x s^2 + B_x s)$, i.e., the desired admittance is achieved. Therefore, we can say that the values of the parameters $\{L, K, B, M\}$ should be chosen so that these conditions are satisfied.

When the plant (16) controlled with (15) is in contact with an elastic surface at the origin, the following relation holds true:

$$f = -K_r q_s \tag{21}$$

where K_r is the stiffness coefficient of the surface. Let us focus on the quantity $f + f_d$, which can be viewed as the error in the contact force in this situation. From (15), (16), and (21), the following relation holds true:

$$\mathcal{L}[f + f_d] = E_2(s)\mathcal{L}[f_d] - E_3(s)\mathcal{L}[f_e] \tag{22}$$

where

$$E_2(s) \triangleq (K_r E_1(s) + 1)/(1 + K_r A(s)) \tag{23}$$

$$E_3(s) \triangleq K_r E_1(s)/(1 + K_r A(s)) \tag{24}$$

$$A(s) \triangleq U_1(s)/(M_x s^2 + B_x s). \tag{25}$$

The denominators of $E_2(s)$ and $E_3(s)$ show that the system composed of (15), (16), and (21) is stable only if the Nyquist plot of $K_r A(j\omega)$ does not encircle the point $-1 + 0j$ in the complex plane. To achieve this property with a higher K_r, the phase lag caused by $U_1(s)$ needs to be set smaller, and thus we can see that $U_1(s) \approx 1$ is desirable also in this case. Because $\lim_{s\to 0} |A(s)| = \infty$, we have $\lim_{s\to 0} E_2(s) = \lim_{s\to 0} E_3(s) = 0$. Therefore, $f + f_d \to 0$ is realized for step inputs in f_d and f_e if this system is stable.

The definitions (18) and (19) imply that, in order to achieve $U_1(s) \approx 1$ and $U_2(s) \approx 1$ in a sufficiently wide range of frequencies, we should not prune the acceleration feedforward term $M\ddot{q}_x$ in the controller (15). It is especially necessary for preventing the phase lag produced by $U_1(s)$, which may cause the instability in the contact with stiff external objects, considering the fact that M_x is usually set smaller than M_r. The necessity of the term $M\ddot{q}_x$ has also been empirically shown in the author's previous paper [8].

This conventional approach to attenuate the contact instability by means of the acceleration feedforward $M\ddot{q}_x$ is also adopted in the proposed methods presented in the subsequent sections. The upcoming Section V-C will discuss some complications caused by the term $M\ddot{q}_x$, but the analysis here implies that this term should not be pruned.

Remark 1: Recalling that the contact with an external object is represented as a feedback loop (21) from q_s to f with the gain K_r, one can see that the system tends to be unstable with a high K_r if the controller and the robot dynamics result in the phase lag of more than $-\pi$ from f to q_s. In the analysis in this section, the phase lag is attributed solely to the transfer function $U_1(s)$. In reality, however, there are other sources of the phase lag, such as the latency in the controller due to the time discretization and the *sensor–actuator noncollocation,* which is the compliance between the force sensor and the actuator [12]–[14]. That is, the above-mentioned analysis depends on the assumption that, roughly speaking, the controller latency is small enough and the member connecting the sensor and the actuator is stiff enough

in comparison to the environment stiffness K_r. Nevertheless, the term $M\ddot{q}_x$ in (15c) can be expected to act as a phase-lead compensator to attenuate the phase lag from f to q_s, as well as the contact instability.

Remark 2: Calanca *et al.*'s review paper [16] provides an overview of force control schemes, including admittance control, with noncollacated devices, such as those with elastic actuators and flexible joints. Kikuuwe *et al.* [15] have presented an analysis on the influence of the sensor-actuator noncollocation due to the joint compliance in a force-projecting master-slave system, which is equivalent to an admittance control system with the proxy replaced by a slave manipulator (see [15, Figs. 1 and 2]). The efficacy of the phase-lead compensator has also been discussed therein. This paper does not attempt to provide new approach to this noncollocation issue, except the inclusion of the simple acceleration feedforward term $M\ddot{q}_x$.

C. Related Work

For an overview on related work on admittance control, readers can refer to [8], which includes brief historical notes and discussion on its relations to explicit force control and impedance control. A more recent review paper [16] discusses a broader class of force control schemes including admittance control.

As has been pointed out in [8], the actuator saturation in admittance control has not attracted much attention. Recent work includes the use of an acceleration limiter [5], [6], which limits the derivatives of the desired position provided to the internal position controller, to avoid the instability caused by the torque saturation. This approach may be similar to the author's previous method [8] in that both of them intend to impose restrictions on the post-saturation behaviors of the robot. A method imposing restrictions on the proxy's motion has also been presented [17], which may somewhat contribute to the prevention of torque saturation. There is another work [18] that employs a neural network to attenuate the tracking error caused by the actuator saturation. Neither of the aforementioned methods explicitly prevents the separation between the proxy's position and the robot's position. Therefore, they do not cope with the case where the robot link is displaced by an external force applied to a portion other than the force sensor.

III. Proposed Controller

A. Continuous-Time Representation

Here, let us assume that we need to impose the constraint $\tau \in \mathcal{F}$ on the controller (15) where $\mathcal{F}$ is a closed interval of real numbers including zero. In order to deal with this case, this paper proposes the following new controller:

$$M_x\ddot{q}_x + B_x\dot{q}_x \in f + f_d - \mathcal{N}_{\mathcal{F}}(\tau) \tag{26a}$$

$$\dot{a} = q_x - q_s \tag{26b}$$

$$\tau = M\ddot{q}_x + K(q_x - q_s) + B(\dot{q}_x - \dot{q}_s) + La. \tag{26c}$$

This set of equations can be seen as a DAI with respect to q_x. Because the normal-cone term $\mathcal{N}_{\mathcal{F}}(\tau)$ does not permit τ outside the set $\mathcal{F}$, the proxy's acceleration $\ddot{q}_x$ is determined so that $\tau \in \mathcal{F}$ is satisfied. As long as τ is in the interior of $\mathcal{F}$, the controller (26) is equivalent to the ordinary admittance controller (15) because $\mathcal{N}_{\mathcal{F}}(\tau) = 0$. A block diagram of the proposed controller (26) is shown in Fig. 1(b), in which the term $\mathcal{N}_{\mathcal{F}}(\tau)$ in (26a) appears as an algebraic feedback loop.

If $\mathcal{F} = [-F, F]$ with a positive constant $F > 0$, the expression (26) can be rewritten as follows:

$$\tau \in -F\mathrm{sgn}(M_x\ddot{q}_x + B_x\dot{q}_x - f - f_d) \tag{27a}$$

$$\dot{a} = q_x - q_s \tag{27b}$$

$$\tau = M\ddot{q}_x + K(q_x - q_s) + B(\dot{q}_x - \dot{q}_s) + La. \tag{27c}$$

Note that (27a) and (27c) constitute a pair of simultaneous equations with two unknowns τ and $\ddot{q}_x$. This controller has some similarity with the author's previous controllers. The expression (27) becomes equivalent to the proxy-based sliding mode controller [9], [10] and its modified version [8] by replacing the argument of sgn in (27a) by other functions of q_x, $\dot{q}_x$, and $\ddot{q}_x$.

One interesting feature of the expression (26), or equivalently (27), is that, through tedious but straightforward derivation using the relation (7), one can equivalently rewrite it by the following ordinary differential equation (ODE):

$$\begin{aligned}\tau = \mathrm{proj}_{\mathcal{F}}\big(&M(f + f_d - B_x\dot{q}_x)/M_x \\ &+ K(q_x - q_s) + B(\dot{q}_x - \dot{q}_s) + La\big)\end{aligned} \tag{28a}$$

$$\ddot{q}_x = (\tau - K(q_x - q_s) - B(\dot{q}_x - \dot{q}_s) - La)/M \tag{28b}$$

$$\dot{a} = q_x - q_s. \tag{28c}$$

It should be cautioned that this ODE (28) is not convenient for implementation because it includes the divisions by M and M_x, which may be very small or even zero. In order to avoid this problem, we need careful discretization of (26), which will be detailed in Section III-B.

B. Proposed Controller: Discrete-Time Representation

A discrete-time representation of the proposed controller (26) is now derived based on the implicit Euler discretization. Let T be the timestep size and k be the integer representing the discrete-time index. By using the implicit Euler discretization, e.g., $\dot{q}_x := (q_x(k) - q_x(k-1))/T$, (26) can be discretized as follows:

$$a(k) = a(k-1) + T(q_x(k) - q_s(k)) \tag{29a}$$

$$\tau(k) = (\hat{K} + M/T^2)\,(q_x(k) - q_s^*(k)) \tag{29b}$$

$$q_x^*(k) - q_x(k) \in \mathcal{N}_{\mathcal{F}}(\tau(k)) \tag{29c}$$

where $\hat{K} \triangleq K + B/T + LT$ and

$$u_x^*(k) \triangleq \frac{M_x u_x(k-1) + T(f(k) + f_d(k))}{M_x + B_x T} \tag{30}$$

$$q_x^*(k) \triangleq q_x(k-1) + Tu_x^*(k) \tag{31}$$

$$\phi_b(k) \triangleq \frac{B(q_x(k-1) - q_s(k-1))}{T} - La(k-1) \tag{32}$$

$$\phi_a(k) \triangleq M\frac{q_s(k) - q_x(k-1) - Tu_x(k-1)}{T^2} \tag{33}$$

$$q_s^*(k) \triangleq q_s(k) + \frac{\phi_b(k) - \phi_a(k)}{\hat{K} + M/T^2} \tag{34}$$

$$u_x(k) \triangleq (q_x(k) - q_x(k-1))/T. \tag{35}$$

By eliminating $q_x(k)$ from (29b) and (29c) by using the relation (7), one obtains the following expression:

$$\tau(k) = \mathrm{proj}_{\mathcal{F}}((\hat{K} + M/T^2)(q_x^*(k) - q_s^*(k))). \tag{36}$$

In conclusions, the proposed controller (26) can be realized in the discrete-time domain as the following algorithm:

$$u_x^*(k) := \frac{M_x u_x(k-1) + T(f(k) + f_d(k))}{M_x + B_x T} \tag{37a}$$

$$q_x^*(k) := q_x(k-1) + T u_x^*(k) \tag{37b}$$

$$\phi_b(k) := \frac{B(q_x(k-1) - q_s(k-1))}{T} - La(k-1) \tag{37c}$$

$$\phi_a(k) := M\frac{q_s(k) - q_x(k-1) - T u_x(k-1)}{T^2} \tag{37d}$$

$$q_s^*(k) := q_s(k) + \frac{\phi_b(k) - \phi_a(k)}{\hat{K} + M/T^2} \tag{37e}$$

$$\tau^*(k) := (\hat{K} + M/T^2)(q_x^*(k) - q_s^*(k)) \tag{37f}$$

$$\tau(k) := \mathrm{proj}_{\mathcal{F}}(\tau^*(k)) \tag{37g}$$

$$q_x(k) := q_s^*(k) + \tau(k)/(\hat{K} + M/T^2) \tag{37h}$$

$$u_x(k) := (q_x(k) - q_x(k-1))/T \tag{37i}$$

$$a(k) := a(k-1) + T(q_x(k) - q_s(k)). \tag{37j}$$

This controller will be referred to as Controller **cP** in subsequent sections.

Note that this algorithm (37) does not involve any set-valued functions or nonclosed-form equations, although its original continuous-time representation (26) involves set-valuedness and differential-algebraic constraints. Although the set-valuedness is not apparent in the algorithm (37), $\tau^*(k) \in \mathcal{F}$ results in $\tau^*(k) = \tau(k)$, $q_x^*(k) = q_x(k)$, and $u_x^*(k) = u_x(k)$, and thus further results in the following:

$$u_x(k) = \frac{M_x u_x(k-1) + T(f(k) + f_d(k))}{M_x + B_x T} \tag{38a}$$

$$\tau(k) = M\frac{u_x(k) - u_x(k-1)}{T} + K(q_x(k) - q_s(k)) + \frac{B(T u_x(k) - (q_s(k) - q_s(k-1))}{T} + La(k) \tag{38b}$$

$$a(k) = a(k-1) + T(q_x(k) - q_s(k)). \tag{38c}$$

Note that this is exactly the discretization of the conventional admittance controller (15). That is, the set-valuedness in the original DAI (26) is implicitly preserved in the algorithm (37) although it is not apparent. The use of the implicit discretization for implicitly preserving the set-valuedness of the original continuous-time representation has been presented by some researchers [19]–[21] including the author and his colleagues [8], [9], [22].

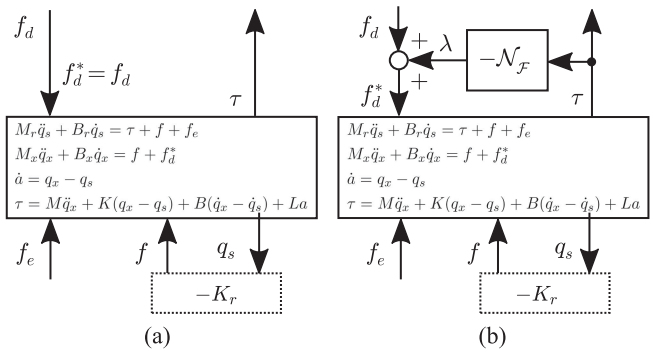

Fig. 3. System composed of (16) and (21) controlled with (a) the conventional controller (15) and (b) the proposed controller (26). The system of (b) comprises a set-valued feedback from τ to λ. (The variable f_d^* is defined here only for the convenience of illustration.)

C. Stability Analysis

The proposed controller (26) can be seen as the interconnection of a linear subsystem

$$M_x\ddot{q}_x + B_x\dot{q}_x = f + f_d + \lambda \tag{39a}$$

$$\dot{a} = q_x - q_s \tag{39b}$$

$$\tau = M\ddot{q}_x + K(q_x - q_s) + B(\dot{q}_x - \dot{q}_s) + La \tag{39c}$$

and a memoryless feedback law

$$\lambda \in -\mathcal{N}_{\mathcal{F}}(\tau) \tag{40}$$

where λ is a newly introduced scalar variable. That is, the controller (26) is equivalently rewritten as (39) and (40). It can be seen that the only difference between the conventional controller (15) and the proposed controller (26) is that f_d in (15) is replaced by $f_d + \lambda$ and the constraint (40) is added in the new controller. Fig. 3 illustrates the relation between the conventional controller (15) and the proposed controller (26), both combined with the plant (16) and the environment (21). With the proposed controller (26), the whole closed-loop system is composed of the nonlinear feedback (40) and the linear subsystem composed of (16), (21), and (39). Because (40) implies $\lambda\tau \leq 0$, the passivity of the linear subsystem is a sufficient condition for the stability of the whole system in Fig. 3(b).

With the subsystem composed of (16) and (39), the relation between the inputs $\{f, f_d, \lambda, f_e\}$ and the output τ can be obtained as follows:

$$\mathcal{L}[\tau] = G_f(s)\mathcal{L}[f] + G_1(s)\mathcal{L}[f_d + \lambda] - U_3(s)\mathcal{L}[f_e] \tag{41}$$

where

$$G_f(s) \triangleq G_1(s) - U_3(s) \tag{42}$$

$$G_1(s) \triangleq \frac{M_r s + B_r}{M_x s + B_x} U_2(s) \tag{43}$$

$$U_3(s) \triangleq \frac{Bs^2 + Ks + L}{M_r s^3 + (B + B_r)s^2 + Ks + L}. \tag{44}$$

From this expression, we have the following result.

Proposition 1: Consider the system (16) combined with the feedback controller (26) with $f = f_e = f_d = 0$. Then, the

origin $[\dot{q}_x, \dot{q}_s, \dot{a}, a]^T = 0$ is globally asymptotically stable if the transfer function $G_1(s)$ defined by (43) is strictly positive real.

Proof: It can be seen that a minimal realization of the transfer function $G_1(s)$ is the system composed of (16) and (39) with the four-dimensional state vector $\boldsymbol{x}_4 \triangleq [\dot{q}_x, \dot{q}_s, \dot{a}, a]^T$, the input λ, the output τ, and $f = f_e = f_d = 0$. If $G_1(s)$ is strictly positive real, there exist positive definite functions $V_4 : \mathbb{R}^4 \to \mathbb{R}$ and $\psi_4 : \mathbb{R}^4 \to \mathbb{R}$ with which $\dot{V}_4(\boldsymbol{x}_4) < \lambda\tau - \psi_4(\boldsymbol{x}_4)$ [23, Lemma 6.4]. Because (40) implies $\lambda\tau \leq 0$, we have $\dot{V}_4(\boldsymbol{x}_4) < 0$ for all $\boldsymbol{x}_4 \neq 0$, which indicates that the system composed of (16), (39), and (40), or equivalently the system composed of (16) and (26), is globally asymptotically stable if $f = f_e = f_d = 0$. ■

When the subsystem composed of (16) and (39) is in contact with an elastic surface as described by (21), the forces f, f_e, and τ are constrained by the following relation:

$$\mathcal{L}[f] = -\frac{K_r(\mathcal{L}[\tau] + \mathcal{L}[f_e])}{M_r s^2 + B_r s + K_r}, \tag{45}$$

which is obtained from (16) and (21). Substituting (45) into (41) shows that the transfer function from the inputs $\{f_d, \lambda, f_e\}$ to τ can be written as follows:

$$\mathcal{L}[\tau] = G_2(s)\mathcal{L}[f_d + \lambda] - G_3(s)\mathcal{L}[f_e] \tag{46}$$

where

$$G_2(s) \triangleq \frac{(M_r s^2 + B_r s + K_r)U_2(s)}{M_x s^2 + B_x s + K_r U_1(s)} \tag{47}$$

$$G_3(s) \triangleq \frac{(M_x s^2 + B_x s)U_3(s) + K_r U_2(s)}{M_x s^2 + B_x s + K_r U_1(s)}. \tag{48}$$

From this expression, we have the following result.

Proposition 2: Consider the system composed of (16) and (21) combined with the feedback controller (26) with $f_e = f_d = 0$. Then, the origin $[\dot{q}_x, \dot{q}_s, \dot{a}, a, q_s]^T = 0$ is globally asymptotically stable if the transfer function $G_2(s)$ defined by (47) is strictly positive real.

Proof: It can be seen that a minimal realization of the transfer function $G_2(s)$ is the system composed of (16), (21), and (39) with the five-dimensional state vector $\boldsymbol{x}_5 \triangleq [\dot{q}_x, \dot{q}_s, \dot{a}, a, q_s]^T$, the input λ, the output τ, and $f_e = f_d = 0$. If $G_2(s)$ is strictly positive real, there exist positive definite functions $V_5 : \mathbb{R}^5 \to \mathbb{R}$ and $\psi_5 : \mathbb{R}^5 \to \mathbb{R}$ with which $\dot{V}_5(\boldsymbol{x}_5) < \lambda\tau - \psi_5(\boldsymbol{x}_5)$ [23, Lemma 6.4]. Because (40) implies $\lambda\tau \leq 0$, we have $\dot{V}_5(\boldsymbol{x}_5) < 0$ for all $\boldsymbol{x}_5 \neq 0$, which indicates that the system composed of (16), (21), (39), and (40), or equivalently, the system composed of (16), (21), and (26), is globally asymptotically stable if $f_e = f_d = 0$. ■

These results indicate that the values of the parameters $\{K, B, L, M, M_x, B_x\}$ need to be chosen so that $G_1(s)$ and $G_2(s)$ are strictly positive real. These functions depend on the functions $U_1(s)$ and $U_2(s)$, which are defined in (19) and (18), respectively. From these definitions, one can see that $K(B + B_r) > LM_r$, $U_1(s) \approx 1$, and $U_2(s) \approx 1$ are necessary for the strict positive realness of $G_1(s)$ and $G_2(s)$. The design of controller parameters to achieve the strict positive realness of $G_1(s)$ and $G_2(s)$ may be possible by using the linear matrix inequality associated with the Kalman–Yakubovic–Popov Lemma [24, Sec. 3.1] if the plant parameters $\{M_r, B_r, K_r\}$ are known. It would be however difficult because the plant parameters are usually unavailable. One practical approach is to set K and B as high as possible, and choose M to be an appropriate value that is close to M_r or $M_r - M_x$.

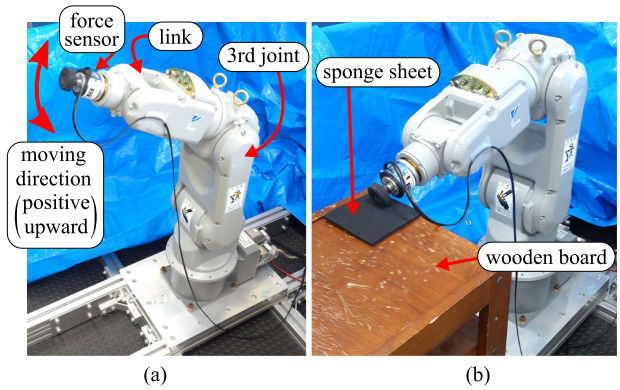

Fig. 4. Setup for experiments. (a) Configuration for Experiment I. (b) Configuration for Experiment II.

Lur'e systems comprising set-valued feedback loops have been investigated by Brogliato and Goeleven [25], focusing on the passivity of the linear parts. The presented results can be seen as simplified cases of the results in [25]. Systems with set-valued feedbacks have also been investigated by Miranda-Villatoro and Castaños [26]. They considered general cases, in which the output is a multidimensional vector and the normal-cone operator is combined with an output regulator. Discrete-time versions of Propositions 1 and 2, which may be obtained in a similar approach to those of Huber *et al.* [27], remain to be addressed.

Remark 3: The analysis in this section is built upon the same assumption as the one in Section II-B, which is that the controller latency and the sensor–actuator noncollocation are negligible. In the same reason as Remark 1 discussed with the conventional admittance controller, the system with the new method tends to be unstable when it is in contact with a stiff external object. The term proportional to M is expected to attenuate the instability due to its effect of phase leading, as it does with the conventional admittance controller. This point will be discussed with the results of experiments in Sections IV-B and V-E.

IV. Experiments

For the validation of the proposed controller (37), the 6-DOF industrial robot MOTOMAN-HP3J (Yaskawa Electric Corporation) shown in Fig. 4 was used. The robot had six ac servomotors, which were integrated with harmonic-drive gearings and optical encoders. A six-axis force sensor (Nitta Corporation) was attached to the end-effector of the robot. A circular holding knob was installed on the force sensor. The whole system was controlled with a PC running the ART-Linux operating system.

The experiments were performed with the third joint of the manipulator, which produced the motion indicated in Fig. 4(a). For the comparison, we used the following three controllers.

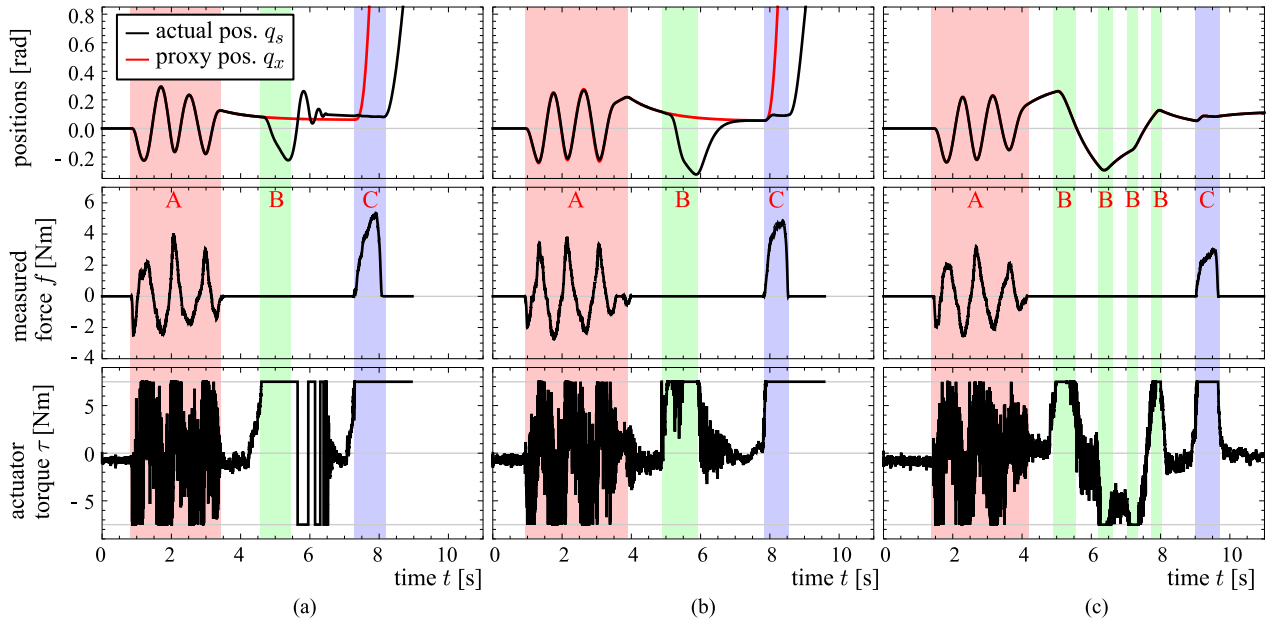

Fig. 5. Results of Experiment I. The experimenter applied forces on the force sensor in Periods A and on the link in Periods B. In Periods C, the experimenter held the link in one hand and applied an upward force on the force sensor by the other hand. (a) Controller **cO**. (b) Controller **cS**. (c) Conroller **cP**.

1) **cO**: The admittance controller consisting of the proxy dynamics (15a) and the following internal position controller:

$$\dot{a} = q_x - q_s \tag{49a}$$

$$\tau = \mathrm{proj}_{\mathcal{F}}(M\ddot{q}_x + K(q_x - q_s) + B(\dot{q}_x - \dot{q}_s) + La), \tag{49b}$$

which is the ordinary torque-saturated PID control.
2) **cS**: The admittance control consisting of the proxy dynamics (15a) and the internal position controller proposed in [8].
3) **cP**: Proposed controller (37).

The parameters were chosen as: $K = 20\,000$ N·m, $B = 140$ N·m·s, $L = 6000$ N·m/s, $M = 3$ kg·m^2, $F = 7.5$ N·m and $\mathcal{F} = [-F, F]$, $M_x = 0.2$ kg·m^2, and $B_x = 0.2$ N·m·s. The gains $\{K, B, L\}$ were chosen as high as the system remained stable, F was set adequately larger than the magnitude of the friction force in the joint, and M was chosen through trial and error. The proxy's parameters $\{M_x, B_x\}$ were chosen as low as the system remained stable with a firm grasping by hand. The timestep size was set as $T = 0.001$ s.

A. Experiment I: Moved by Hand

In the first set of experiments, the robot was moved by the experimenter's hand through the holding knob. The desired force f_d was set zero. The results are shown in Fig. 5. In Periods A, the experimenter moved the robot by grasping the force sensor. In Periods B, the experimenter applied the force on the link, not on the force sensor. In Periods C, the experimenter held the link so that it should not move and applied an upward (positive) force on the force sensor.

In Periods A, all controllers realized appropriate admittance control, in which the proxy and robot positions well coincide with each other. In Periods B, when a force was applied to the link, the proxy did not move with **cO** and **cS** but it followed the robot with **cP**. The separation between the proxy and the robot produced by **cO** and **cS** resulted in snapping-back motions after Periods B. The motion produced by **cO** was overshooting and oscillatory, whereas that produced by **cS** was rather smooth and monotonic, due to the effect of the internal position controller proposed in [8]. With the new controller **cP**, in contrast, the proxy followed the robot in Periods B, after which there was no snapping-back motion. (Fig. 5(c) includes several Periods B because the experimenter pushed the link several times to move it back to the original position.)

In Periods C, i.e., when an upward force was applied to the force sensor and the link was held unmoved, **cO** and **cS** resulted in the proxy's moving away from the robot in the positive (upward) direction. In the same situation, **cP** did not produce such a proxy motion. After Periods C, when the experimenter released the hands from the robot, **cO** and **cS** drove the robot to catch up with the proxy that was already far separated. It is clearly undesirable and unsafe behavior. Such behaviors were not seen in the proposed controller **cP**.

B. Experiment II: Contact With Environment

Another set of experiments was performed to test the stability of the proposed controller in contact with a stationary external object. Specifically, it was to test the efficacy of the acceleration feedforward term (with the coefficient $M > 0$), which is for improving the contact stability, as has been discussed in Section II-B. As shown in Fig. 4(b), a sponge sheet was placed on a wooden board in front of the robot and the third joint was

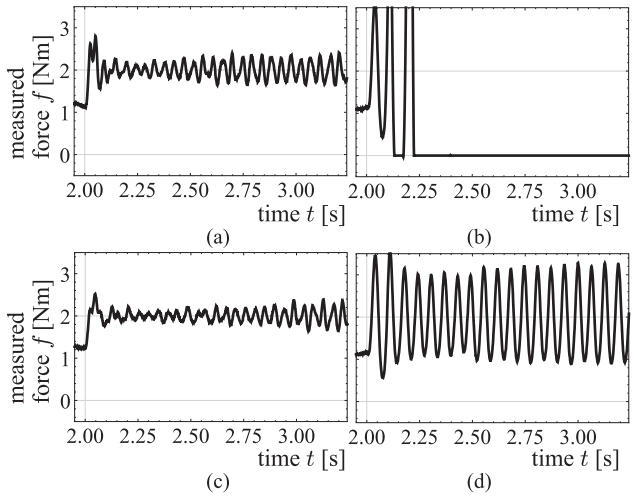

Fig. 6. Results of Experiment II. The admittance controller started at $t = 2$ s. (a) Controller **cO**. (b) Controller **cOo**. (c) Controller **cP**. (d) Controller **cPo**. The suffix **o** attached to the controllers' names indicates $M = 0$.

controlled to push the sponge sheet downward with its end-effector. A position controller was initially used to hold the end-effector lightly in contact with the sponge sheet, and at the time $t = 2$ s, it was switched to an admittance controller with a constant force command $f_d = -2$ N·m. The admittance controllers **cO** and **cP** and those with $M = 0$, denoted by **cOo** and **cPo**, respectively, were used.

The results are shown in Fig. 6. The controller **cOo** resulted in bouncing and jumping, whereas the other three controllers maintained the contact with the surface, although the controller **cPo** produced vibratory contact force. It is clearly seen that the acceleration feedforward ($M > 0$) contributes to the contact stability not only with the conventional controller **cO** but also with the proposed controller **cP**. These results support the efficacy and the necessity of the acceleration feedforward term with $M > 0$ in the proposed controller. It can also be observed that, without the acceleration feedforward (i.e., $M = 0$), the proposed controller **cPo** realizes better stability than the conventional one **cOo**, although the proposed technique is not intended to improve the contact stability. This difference can be attributed to the fact that **cPo** prevents the separation of the proxy from the actual position.

In these experiments, the sponge sheet was used to stabilize the contact with the same parameter values as those in Experiment I. In the direct contact with the wooden board, the system was destabilized with the bouncing behavior both with the conventional and proposed controllers. Even with the sponge sheet, small oscillatory behaviors are still observed in the results of **cP** and **cO** in Fig. 6(a) and (c). These bouncing and oscillatory behaviors can be reduced if one is allowed to set the desired inertia M_x and the desired viscosity B_x higher. As discussed in Remarks 1–3, such unstable behaviors are attributed to the phase lag caused by $U_1(s)$, the time discretization of the controller, and also to the sensor-actuator noncollocation due to the compliance of the joint transmissions. The condition $K(B + B_r) > LM_r$ mentioned in Section III-C is supposed to be unrelated because $L = 0$ also results in bouncing or oscillation.

V. Some Modifications

This section presents three modifications on the controller (37), of which the continuous-time representation is (26). These modifications are not within the scope of the analysis in Section III-C, but have been found useful through experiments. Sections V-A–V-C will present the modifications and Sections V-D and V-E will show the results of some experiments.

A. Modification A: Including Proxy's Coulomb Friction

One practical drawback of the controller (37), or equivalently (26), is that, because of the linear proxy dynamics (26a), the robot starts to drift even with a small force on the force sensor, and it does not exactly stop in finite time but may decelerate only exponentially. If one needs to remove these features, one straightforward idea is to include a Coulomb friction term in the proxy dynamics, which extends the controller (26) into the following form:

$$M_x\ddot{q}_x + B_x\dot{q}_x \in -F_x\mathrm{sgn}(\dot{q}_x) + f + f_d - \mathcal{N}_{\mathcal{F}}(\tau) \quad (50a)$$

$$\dot{a} = q_x - q_s \quad (50b)$$

$$\tau = M\ddot{q}_x + K(q_x - q_s) + B(\dot{q}_x - \dot{q}_s) + La. \quad (50c)$$

Here, $F_x > 0$ is the magnitude of the Coulomb friction force to which the proxy is subject. Note that (50a) includes two set-valued functions in the right-hand side and it should be understood according to the rule (12). If $\mathcal{F} = [-F, F]$, it can be equivalently rewritten as follows:

$$\tau \in -F\mathrm{sgn}(M_x\ddot{q}_x + B_x\dot{q}_x + F_x\mathrm{sgn}(\dot{q}_x) - f - f_d), \quad (51)$$

which includes two sgn functions in a nested way and it should be understood according to the rule (14).

With the implicit Euler discretization of (50), one obtains a set of algebraic inclusions with two set-valued functions. It can be analytically solved through the derivation presented in the appendix. The resultant algorithm is the one obtained by replacing the line (37a) of the proposed controller (37) by the following line:

$$u_x^*(k) := \mathrm{dzn}_{\mathcal{V}_x}\left(\frac{M_x u_x(k-1) + T(f(k) + f_d(k))}{M_x + B_x T}\right) \quad (52)$$

where

$$\mathcal{V}_x \triangleq \left[-\frac{TF_x}{M_x + B_x T}, \frac{TF_x}{M_x + B_x T}\right]. \quad (53)$$

An admittance controller including Coulomb friction has been presented by Kikuuwe *et al.* [22], where the implicit Euler discretization has also been used. A nested signum structure, similar to (51), has been investigated by Miranda-Villatoro *et al.* [28], who provided a rigorous analysis in terms of the uniqueness and existence of the solution in the continuous-time domain. The presented modification, injecting additional Coulomb friction, should not be confused with the compensation techniques for joint friction [29], [30], which have been shown to enhance the stability of admittance control [31]. The influence of the additional Coulomb friction on the closed-loop stability would need

an extension of the analysis in Section III-C, which is left outside the scope of this paper.

B. Modification B: Preventing Saturation-Induced Kinetic Energy Injection

One feature of the proposed controller (37) is that the actuator saturation may inject kinetic energy to the robot. When the robot is moved by an external force and the actuator torque is saturated, the proxy follows the robot's movement and gains a velocity $u_x(k)$. This velocity $u_x(k)$ is then used to calculate the proxy position $q_x(k+1)$ of the next timestep. This means that, when the actuator is saturated, the work done by the external force is stored as the kinetic energy of the proxy, as well as that of the robot. This feature may be undesirable for safety reasons.

As indicated in the line (37a) of the algorithm (37), $u_x^*(k)$ is determined only by the predefined dynamics of the proxy, and thus it can be referred to as the *pre-saturation* proxy velocity. Meanwhile, $u_x(k)$ can be referred to as the *post-saturation* proxy velocity because it is determined by the pre-saturation velocity $u_x^*(k)$ plus the saturation effect. Therefore, one way to prevent the kinetic energy injection done by the actuator saturation is to determine $u_x(k)$ so that it satisfies $u_x(k) \in \mathrm{co}(\{0, u_x^*(k)\})$, which indicates that the saturation only dissipates the proxy's kinetic energy and that the direction of $u_x^*(k)$ is preserved in $u_x(k)$. This idea can be realized by replacing the line (37i) of the algorithm (37) by the following line:

$$u_x(k) := \mathrm{proj}_{\mathrm{co}(\{0,u_x^*(k)\})}\left((q_x(k) - q_x(k-1))/T\right). \quad (54)$$

Note that this modification does not affect the current proxy position $q_x(k)$, but does modify only the proxy velocity $u_x(k)$, which influences the proxy position $q_x(k+1)$ in the next timestep. The underlying idea is that the proxy position $q_x(k)$ needs to be consistent with the torque $\tau(k)$ but the proxy velocity, which is an independent state variable, does not need to satisfy $u_x(k) = (q_x(k) - q_x(k-1))/T$.

C. Modification C: Pre-saturation Acceleration Feedforward

As has been discussed in Section II-B, the acceleration feedforward term, which is the term $M\ddot{q}_x$ in the internal position controller (15c) or (26c), enhances the stability of admittance-controlled systems. Such an effect has also been supported by results of experiments in Section IV-B and those in a previous paper [8]. With some preliminary experiments, however, it has been observed that the term $M\ddot{q}_x$ combined with Modification B in Section V-B causes problematic behaviors of the robot. Such results will be shown in Section V-D.

This section provides a workaround for this problem, of which the efficacy will be shown through the experiments in Section V-D. Considering that the term $M\ddot{q}_x$ in (26c) is the source of problematic behaviors under the saturation, we consider replacing it by a quantity that is not affected by the actuator saturation. With a somewhat abusive mathematical notation, we here consider the following variant of the controller (26):

$$M_x\ddot{q}_x^* + B_x\dot{q}_x = f + f_d \quad (55a)$$

$$M_x\ddot{q}_x + B_x\dot{q}_x \in f + f_d - \mathcal{N}_{\mathcal{F}}(\tau) \quad (55b)$$

$$\dot{a} = q_x - q_s \quad (55c)$$

$$\tau = \mathrm{proj}_{\mathcal{F}}(M\ddot{q}_x^*) + K(q_x - q_s) + B(\dot{q}_x - \dot{q}_s) + La. \quad (55d)$$

The difference between this controller and the original one (26) appears in the feedforward term in (55d). Here, the quantity $\ddot{q}_x^*$ can be seen as a *pre-saturation* acceleration that could have been achieved if the actuator saturation did not happen. The projection operator imposed on the term $M\ddot{q}_x^*$ in (55d) is to prevent the term from becoming excessively large even when a large impulsive force is applied to the force sensor.

In the algorithm (37) and its variants in the previous sections, the quantity $u_x^*(k)$ is the proxy's *pre-saturation* velocity that could have been achieved if the saturation did not happen. Therefore, it is reasonable to set the following relation:

$$\ddot{q}_x^* \approx (u_x^*(k) - u_x(k-1))/T. \quad (56)$$

By using this, one can discretize (55) as follows:

$$a(k) = a(k-1) + T(q_x(k) - q_s(k)) \quad (57a)$$

$$\tau(k) = \hat{K}\left(q_x(k) - q_s^*(k)\right) \quad (57b)$$

$$q_x^*(k) - q_x(k) \in \mathcal{N}_{\mathcal{F}}(\tau(k)) \quad (57c)$$

where

$$u_x^*(k) \triangleq \frac{M_x u_x(k-1) + T(f(k) + f_d(k))}{M_x + B_x T} \quad (58)$$

$$q_x^*(k) \triangleq q_x(k-1) + T u_x^*(k) \quad (59)$$

$$\phi_b(k) \triangleq \frac{B(q_x(k-1) - q_s(k-1))}{T} - La(k-1) \quad (60)$$

$$\phi_a(k) \triangleq \mathrm{proj}_{\mathcal{F}}(M(u_x^*(k) - u_x(k-1))/T) \quad (61)$$

$$q_s^*(k) \triangleq q_s(k) + (\phi_b(k) - \phi_a(k))/\hat{K} \quad (62)$$

$$u_x(k) \triangleq (q_x(k) - q_x(k-1))/T. \quad (63)$$

The definitions of $u_x^*(k)$, $q_x^*(k)$, $\phi_b(k)$, and $u_x(k)$ are not altered from the original ones in (37). In the same light as the derivation from (29) to (37), one can analytically solve the algebraic relation (57) by using the relation (7) and can finally arrive at the algorithm that is identical to (37) except the lines (37d)–(37h) replaced by the following lines:

$$\phi_a(k) := \mathrm{proj}_{\mathcal{F}}(M(u_x^*(k) - u_x(k-1))/T) \quad (64a)$$

$$q_s^*(k) := q_s(k) + (\phi_b(k) - \phi_a(k))/\hat{K} \quad (64b)$$

$$\tau^*(k) := \hat{K}(q_x^*(k) - q_s^*(k)) \quad (64c)$$

$$\tau(k) := \mathrm{proj}_{\mathcal{F}}(\tau^*(k)) \quad (64d)$$

$$q_x(k) := q_s^*(k) + \tau(k)/\hat{K}. \quad (64e)$$

That is, the modification proposed here is to replace the lines (37d)–(37h) of the algorithm (37) by the lines (64).

The whole algorithm after the three modifications in Sections V-A–V-C is presented as follows:

$$u_x^*(k) := \mathrm{dzn}_{\mathcal{V}_x}\left(\frac{M_x u_x(k-1) + T(f(k)+f_d(k))}{M_x + B_x T}\right) \quad (65a)$$

$$q_x^*(k) := q_x(k-1) + T u_x^*(k) \quad (65b)$$

$$\phi_b(k) := \frac{B(q_x(k-1) - q_s(k-1))}{T} - La(k-1) \quad (65c)$$

$$\phi_a(k) := \mathrm{proj}_{\mathcal{F}}(M(u_x^*(k) - u_x(k-1))/T) \quad (65d)$$

$$q_s^*(k) := q_s(k) + (\phi_b(k) - \phi_a(k))/\hat{K} \quad (65e)$$

$$\tau^*(k) := \hat{K}(q_x^*(k) - q_s^*(k)) \quad (65f)$$

$$\tau(k) := \mathrm{proj}_{\mathcal{F}}(\tau^*(k)) \quad (65g)$$

$$q_x(k) := q_s^*(k) + \tau(k)/\hat{K} \quad (65h)$$

$$u_x(k) := \mathrm{proj}_{\mathrm{co}(\{0, u_x^*(k)\})}\left((q_x(k) - q_x(k-1))/T\right) \quad (65i)$$

$$a(k) := a(k-1) + T(q_x(k) - q_s(k)). \quad (65j)$$

This algorithm (65) will be referred to as Controller **cPABC** in subsequent sections. This modified algorithm (65) may be more convenient than the original one (37) for some applications, although it has not yet been theoretically supported. One difficulty in the analysis is that the modified algorithm (65) does not have a continuous-time counterpart in contrast to the fact that the original algorithm (37) has the continuous-time counterpart (26). Another important fact is that, as long as the actuator is not saturated, i.e., $\tau^*(k) \in \mathcal{F}$, the modified algorithm (65) is analytically equivalent to the implicit Euler discretization of the conventional admittance controller including Coulomb friction, which is described as follows:

$$M_x \ddot{q}_x + B_x \dot{q}_x \in -F_x \mathrm{sgn}(\dot{q}_x) + f + f_d \quad (66a)$$

$$\dot{a} = q_x - q_s \quad (66b)$$

$$\tau = M\ddot{q}_x + K(q_x - q_s) + B(\dot{q}_x - \dot{q}_s) + La. \quad (66c)$$

That is, the feedforward term $M\ddot{q}_x$ is still active as long as the actuator is not saturated.

D. Experiment III: Moved by Hand

Some experiments were performed with the modifications presented in the last sections. The same setup as in Section IV was used. The following six controllers were used.

1) **cP**: The algorithm (37), which is the basic form of the proposed controller.
2) **cPA**: Controller **cP** plus Modification A (proxy's Coulomb friction), which is the algorithm (37) with (37a) replaced by (52).
3) **cPB**: Controller **cP** plus Modification B (prevention of saturation-induced kinetic energy), which is the algorithm (37) with (37i) replaced by (54).
4) **cPBo**: Controller **cPB** with $M = 0$ (no acceleration feedforward).
5) **cPBC**: Controller **cPB** plus Modification C (pre-saturation acceleration feedforward), which is the algorithm (65) with $F_x = 0$ (no proxy's Coulomb friction).
6) **cPABC**: The algorithm (65), which includes all three modifications.

The parameters were the same as the experiments in Section IV except that the proxy's friction force is set as $F_x = 0.2$ N·m with **cPA** and **cPABC**. Controller **cPBo** was included to show that $M > 0$ is the source of problematic behaviors of Modification B.

In the experiments, the experimenter pushed the force sensor upward, and then pushed the link downward. The results are shown in Fig. 7. The periods of upward pushing on the force sensor are indicated as Periods A and the periods of downward pushing on the link are indicated as Periods B.

With Controller **cP**, the robot continued moving both after Periods A and B with slight deceleration. The continued motions can be explained by the proxy's storing the work done by the forces both on the force sensor and on the link. With Controller **cPA**, the robot also continued moving for a while after these two periods, but decelerated non-exponentially and ceased to move eventually. These behaviors exhibit the effect of the proxy's Coulomb friction introduced as Modification A.

A problematic behavior took place with Controller **cPB**. As can be seen in Fig. 7(c), in Period B, **cPB** produced a separation between the robot's position q_s and the proxy's position q_x. After this period, the separation caused a snapping-back motion, followed by some oscillation. This undesirable behavior is removed with **cPBo** and **cPBC**. Controllers **cPBo** and **cPBC** realized almost the same motion as **cP** after Period A, but almost immediately stopped after Period B, which was the motion intended in Modification B. Therefore, one can see that $M > 0$ is the source of the problematic behavior of **cPB** and it is removed by setting $M = 0$ or by Modification C.

One possible explanation on the cause of the problem of **cPB** is presented as follows. The algorithm (37) implies that

$$\tau(k) = \hat{K}(q_x(k) - q_s(k)) - \phi_b(k) + M(q_x(k) - q_x(k-1) - T u_x(k-1))/T^2 \quad (67)$$

is satisfied where $\phi_b(k)$ is defined as in (32). When $\tau(k)$ is saturated as $\tau(k) = F$ and $u_x(k-1)$ is set as $u_k(k-1) \approx 0$ as the effect of Modification B, (67) becomes as follows:

$$F \approx \hat{K}(q_x(k) - q_s(k)) - \phi_b(k) + M\frac{q_x(k) - q_x(k-1)}{T^2}. \quad (68)$$

In this situation, the proxy position $q_x(k)$ is determined according to the input $q_s(k)$ and the relation (68), and the last term proportional to M injects a strong damping in the proxy motion with the viscosity coefficient of M/T. The value of M/T is 3000 N·m·s in this experiment and is much larger than the derivative gain $B = 140$ N·m·s. Therefore, the separation between $q_x(k)$ and $q_s(k)$ with **cPB** is attributed to the damping produced by the last term of (68), which prevents the proxy from following the robot. The motion of the proxy in Fig. 7(c) is consistent with this explanation.

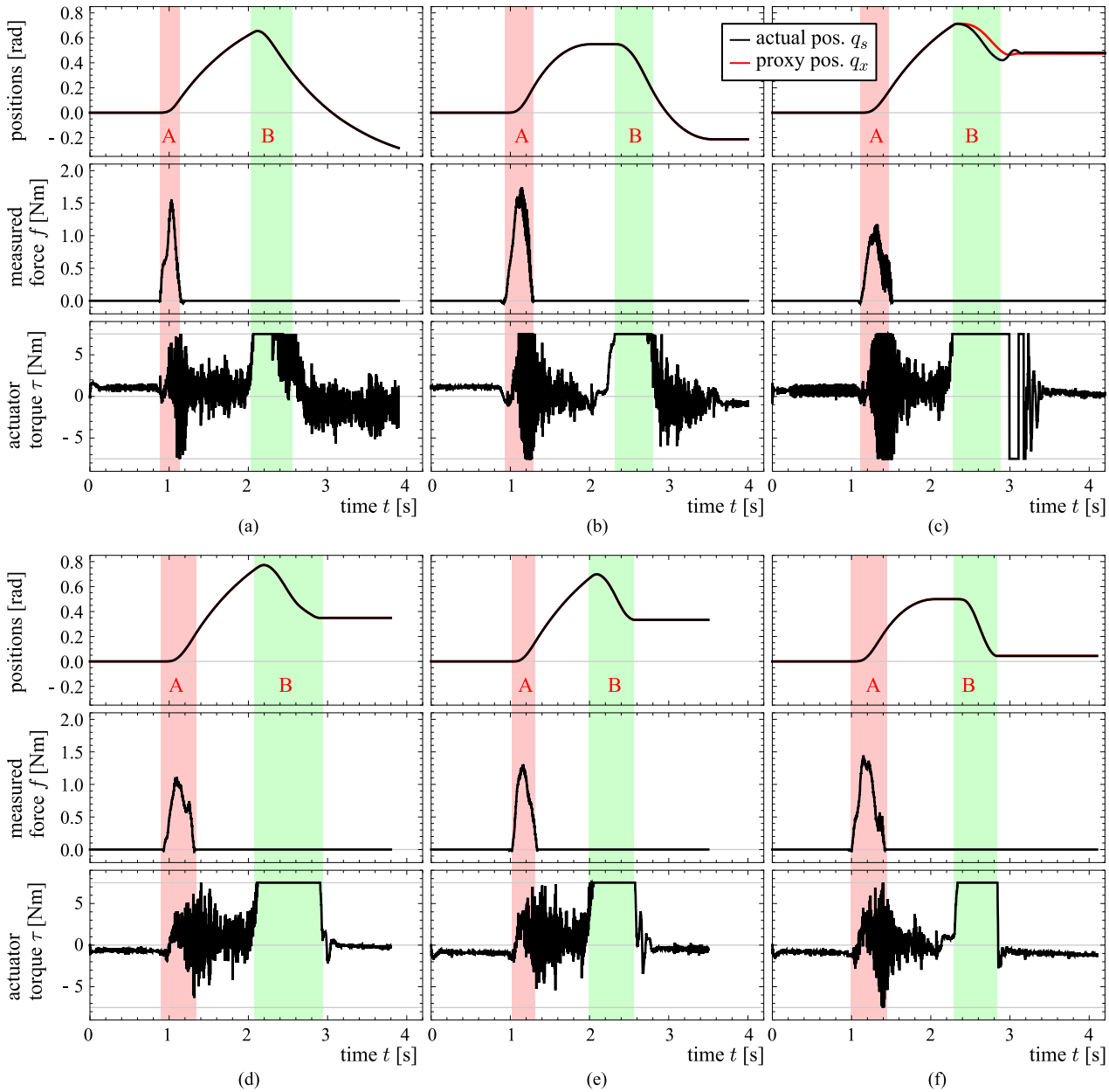

Fig. 7. Results of Experiment III, with modified versions of the proposed controller. The actual position and the proxy position are almost overlapping except (c). The experimenter applied a force on the force sensor during Periods A and on the link during Periods B. (a) Controller **cP**. (b) Controller **cPA**. (c) Controller **cPB**. (d) Controller **cPBo**. (e) Controller **cPBC**. (f) Controller **cPABC**.

The fully modified version **cPABC**, which is the algorithm (65), showed intended features of both Modifications A and B, which are the smooth and non-exponential halting after Period A and the immediate stop after Period B.

E. Experiments IV and V: Contact With Environment

The modified controllers were also tested in contact with a stationary object in another set of experiments, Experiment IV. The experiments were performed in the same way as Experiment II and the setup was used as shown in Fig. 4(b). Four controllers, **cPBo**, **cPBC**, **cPABC**, and **cPABCo**, where the suffix **o** stands for $M = 0$, were used to clarify the effectiveness of the acceleration feedforward combined with the presented modifications.

Fig. 8 shows the results. The comparison between **cPBo** and **cPBC** shows that the acceleration feedforward is effective also with Modification B when it is combined with Modification C. The absence of Modification C, i.e., **cPB**, was not tested because it is already shown to be problematic in Experiment III. The latter two controllers, **cPABC** and **cPABCo**, show that Modification A (the proxy's Coulomb friction) is more effective than the acceleration feedforward to improve the contact stability. The difference between **cPABC** and **cPABCo** appeared in the transient response, in which **cPABC** was smoother than **cPABCo**. Due to the proxy's

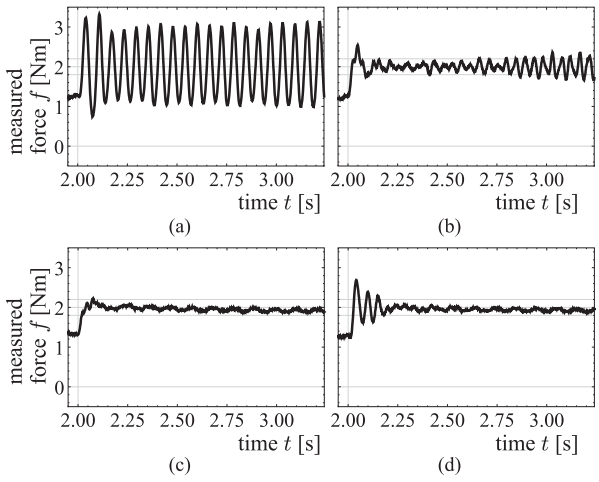

Fig. 8. Results of Experiment IV: contact with a soft surface (sponge sheet). (a) Controller **cPBo**. (b) Controller **cPBC**. (c) Controller **cPABC**. (d) Controller **cPABCo**. The suffix **o** means $M = 0$.

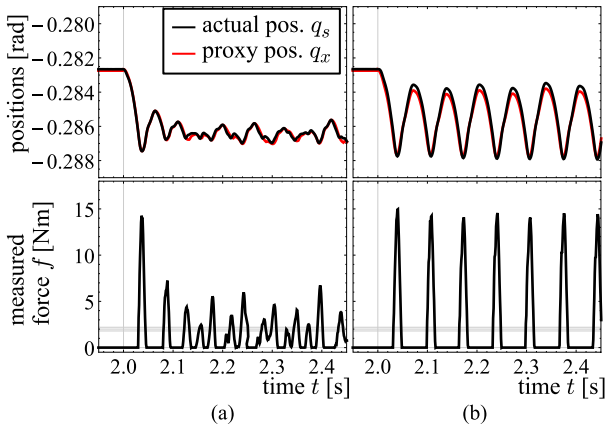

Fig. 9. Results of Experiment V: contact with a hard surface (wooden board). (a) Controller **cPABC**. (b) Controller **cPABCo**. The suffix **o** means $M = 0$.

Coulomb friction, the contact force f is expected to converge to the interval $-f_d + [-F_x, F_x] = [1.8\ \text{N·m}, 2.2\ \text{N·m}]$. Fig. 8(c) and (d) shows that f became almost stationary within this range.

Because the difference between **cPABC** and **cPABCo** was not very apparent in contact with a sponge sheet, another set of experiments, Experiment V, was performed with a stiffer (i.e., more destabilizing) environment. The sponge sheet was removed and the robot was made directly in contact with the wooden board indicated in Fig. 4(b). Fig. 9 shows the results. It shows that, with both controllers, the end-effector exhibited continued bouncing on the environment surface and failed to establish stable contact. Comparing these two, one can see that the bouncing of **cPABC** is smaller than that of **cPABCo**, indicating that the acceleration feedforward is effective even in combination with Modification A. Again, the source of this instability can be supposed to be those discussed in Remarks 1–3. It should also be noted that this bouncing can be removed if one is allowed to increase the desired inertia M_x and the desired viscosity B_x.

A conclusion drawn from the experiments is that, from a practical point of view, the fully modified version **cPABC** is most recommended, although its properties have not been fully clarified from a theoretical point of view. The unmodified controller **cP** may be recommended if one needs controllers of which the properties are theoretically clarified.

VI. Conclusion

This paper has proposed a new admittance controller that operates with a bounded actuator torque. It is analytically equivalent to a conventional admittance controller as long as the actuator is not saturated, but it behaves safely even when the actuator torque is saturated, without producing the separation between the proxy position and the robot position. The continuous-time representation of the proposed controller is given as a DAI, which includes a set-valued function. The discrete-time implementation has been derived through the implicit Euler discretization of the DAI, and the resultant algorithm is of the closed form and free from the set-valuedness. In addition to the proposed DAI-based controller, some modifications have been presented to alleviate practical inconveniences of the proposed controller. Although theoretical properties of these modifications have not yet been clarified, the efficacy of the modifications is supported with the results of some experiments.

Conventional admittance controllers produce unpredictable behaviors when the proxy position is separated from the robot position. Therefore, admittance-controlled robots had to be prevented from gaining contact with external objects at portions other than the force sensor. The proposed controller casts aside such concerns, and thus is expected to be useful for force control applications in human-centered environments where the safety is of utmost importance.

This paper has assumed the use of a force sensor on the end-effector. The proposed technique would be useful to cope with the actuator saturation also in combination with sensorless admittance control, e.g., [32] and [33], using some means to estimate external forces.

Future study should address theoretical details on the presented modifications on the controller. Multidimensional implementation of the proposed algorithms, e.g., admittance control in the Cartesian task space with joint torque limits, is also an important topic for industrial and human-centered applications.

Appendix

The process of discretizing (50) to obtain (52) is presented here. The following lemmas are useful for this purpose.

Lemma 1: With $x \in \mathbb{R}$, $y \in \mathbb{R}$, and $F > 0$, the following two statements hold true:

$$x - F\mathrm{sgn}(y - x) - [0, \infty) \ni 0 \iff x \geq \mathrm{proj}_{[-F,F]}(y)$$
$$x - F\mathrm{sgn}(y - x) - (-\infty, 0] \ni 0 \iff x \leq \mathrm{proj}_{[-F,F]}(y).$$

Proof: The first statement is proven as follows:

$$\begin{aligned} & x - F\mathrm{sgn}(y - x) - [0, \infty) \ni 0 \\ & \iff (x - F \geq 0 \ \wedge \ y > x) \vee (x + F \geq 0 \ \wedge \ y \leq x) \\ & \iff F \leq x < y \ \vee \ x \geq \max(-F, y) \end{aligned}$$

$$\begin{aligned}
&\iff F \le x < \max(-F, y) \ \vee \ x \ge \max(-F, y) \\
&\iff x \ge \min(F, \max(-F, y)) \\
&\iff x \ge \mathrm{proj}_{[-F,F]}(y). \qquad (69)
\end{aligned}$$

The second statement is proven in a similar way to (69). ■

Lemma 2: With $x \in \mathbb{R}$, $a \in \mathbb{R}$, $b \in \mathbb{R}$, $A > 0$, and a closed set $\mathcal{F} \subset \mathbb{R}$, the following statement holds true:

$$\begin{aligned}
&x + \mathcal{N}_{\mathcal{F}}(x) + A\mathrm{sgn}(x+b) \ni a \\
&\quad \iff x = \mathrm{proj}_{\mathcal{F}}\left(\mathrm{dzn}_{[-A,A]}(a+b) - b\right). \qquad (70)
\end{aligned}$$

Proof: Let us define the following set-valued function $\beta : \mathbb{R} \times \mathbb{R} \times \mathbb{R} \rightrightarrows \mathbb{R}$:

$$\beta(x, a, b) \triangleq a - x - A\mathrm{sgn}(x+b). \qquad (71)$$

Then, we have the following:

$$\begin{aligned}
\beta(x,a,b) \ni 0 &\iff a - x \in A\mathrm{sgn}(x+b) \\
&\iff a - x \in A\mathrm{sgn}(b + a - (a - x)) \\
&\iff a - x = \mathrm{proj}_{[-A,A]}(a+b) \\
&\iff \hat{\beta}(x,a,b) = 0 \qquad (72)
\end{aligned}$$

where $\hat{\beta}(x,a,b)$ is a single-valued function defined as follows:

$$\hat{\beta}(x,a,b) \triangleq -x - b + \mathrm{dzn}_{[-A,A]}(a+b). \qquad (73)$$

Moreover, an analysis employing Lemma 1 shows that the following two statements hold true:

$$\beta(x,a,b) - [0, +\infty) \ni 0 \iff \hat{\beta}(x,a,b) \ge 0 \qquad (74)$$

$$\beta(x,a,b) - (-\infty, 0] \ni 0 \iff \hat{\beta}(x,a,b) \le 0. \qquad (75)$$

These three relations (72), (74), and (75) can be written in the following unified expression:

$$\begin{aligned}
&\forall \mathcal{X} \in \{\{0\}, [0,\infty), (-\infty, 0]\}, \\
&\quad \mathcal{X} - \beta(x,a,b) \ni 0 \iff \mathcal{X} - \hat{\beta}(x,a,b) \ni 0. \qquad (76)
\end{aligned}$$

Considering that $\mathcal{N}_{\mathcal{F}}(x)$ takes only the three set values $\{0\}$, $[0,\infty)$, and $(-\infty, 0]$, one can see that the following is satisfied:

$$\begin{aligned}
&x + \mathcal{N}_{\mathcal{F}}(x) + A\mathrm{sgn}(x+b) \ni a \\
&\quad \iff \mathcal{N}_{\mathcal{F}}(x) - \beta(x,a,b) \ni 0 \\
&\quad \iff \mathcal{N}_{\mathcal{F}}(x) - \hat{\beta}(x,a,b) \ni 0 \\
&\quad \iff \mathcal{N}_{\mathcal{F}}(x) + x + b - \mathrm{dzn}_{[-A,A]}(a+b) \ni 0 \\
&\quad \iff x = \mathrm{proj}_{\mathcal{F}}\left(\mathrm{dzn}_{[-A,A]}(a+b) - b\right). \qquad (77)
\end{aligned}$$

■

Now, let us start with (50). The difference between (50) and (26) is the term $F_x\mathrm{sgn}(u_x(k))$ added to the same place as $\mathcal{N}_{\mathcal{F}}(\tau(k))$. Noting that (26) is discretized into (29), (50) is discretized in the following form:

$$a(k) = a(k-1) + T(q_x(k) - q_s(k)) \qquad (78a)$$

$$\tau(k) = (\hat{K} + M/T^2)\,(q_x(k) - q_s^*(k)) \qquad (78b)$$

$$q_x^{**}(k) - q_x(k) \in \mathcal{N}_{\mathcal{F}}(\tau(k)) + TV_x\mathrm{sgn}(u_x(k)) \qquad (78c)$$

where $\hat{K} \triangleq K + B/T + LT$, $V_x \triangleq TF_x/(M_x + B_xT)$

$$u_x(k) \triangleq (q_x(k) - q_x(k-1))/T \qquad (79)$$

$$q_x^{**}(k) \triangleq q_x(k-1) + Tu_x^{**}(k) \qquad (80)$$

$$u_x^{**}(k) \triangleq \frac{M_x u_x(k-1) + T(f(k) + f_d(k))}{M_x + B_xT} \qquad (81)$$

and $q_s^*(k)$ is the one defined in (34). Eliminating $q_x(k)$ and $u_x(k)$ from (78b), (78c), and (79) yields the following:

$$\begin{aligned}
&q_x^{**}(k) - q_s^*(k) - \frac{\tau(k)}{\hat{A}} \in \\
&\quad \mathcal{N}_{\mathcal{F}}(\tau(k)) + TV_x\mathrm{sgn}\left(\frac{\tau(k)}{\hat{A}} + q_s^*(k) - q_x(k-1)\right) \qquad (82)
\end{aligned}$$

where $\hat{A} = \hat{K} + M/T^2$. Lemma 2 suggests that it is rewritten as follows:

$$\begin{aligned}
\tau(k) &= \mathrm{proj}_{\mathcal{F}}\big(\mathrm{dzn}_{[-T\hat{A}V_x, T\hat{A}V_x]}(\hat{A}(q_x^{**}(k) - q_x(k-1))) \\
&\qquad - \hat{A}(q_s^*(k) - q_x(k-1))\big) \\
&= \mathrm{proj}_{\mathcal{F}}\big(\hat{A}(Tu^*(k) + q_x(k-1) - q_s^*(k))\big) \qquad (83)
\end{aligned}$$

where

$$u^*(k) \triangleq \mathrm{dzn}_{[-V_x, V_x]}\left((q_x^{**}(k) - q_x(k-1))/T\right). \qquad (84)$$

A careful examination shows that (84) is equivalent to (52) and that (83) is equivalent to (37g) substituted by (37b) and (37f). Therefore, one can see that the solution of (78) is obtained by the algorithm (37) with $u_x^*(k)$ replaced by the one in (52).

Some additional remarks follow:

Remark 4: The function $\hat{\beta}(x,a,b)$ introduced in the proof of Lemma 2 plays a similar role to complementarity functions (C-functions) [34, Sec. 1], such as the Fischer–Burmeister function [35]–[37], for nonlinear complementarity problems. With the property (76), the single-valued function $\hat{\beta}(x,a,b)$ can be used to replace the set-valued function $\beta(x,a,b)$ to simplify the problem.

Remark 5: The nested sign structure shown in (51) should be read as follows:

$$\begin{aligned}
&b \in \mathrm{sgn}(x + \mathrm{sgn}(a)) \\
&\quad \iff \exists \eta \in \mathrm{sgn}(a) \text{ s.t. } b \in \mathrm{sgn}(x + \eta) \\
&\quad \iff \exists \eta \in \mathrm{sgn}(a) \text{ s.t. } \mathcal{N}_{[-1,1]}(b) \ni x + \eta \\
&\quad \iff \mathcal{N}_{[-1,1]}(b) - \mathrm{sgn}(a) \ni x, \qquad (85)
\end{aligned}$$

which justifies the equivalence between (51) and (50a). The derivation in (85) employs the fact (13).

ACKNOWLEDGMENT

The author would like to thank Dr. B. Brogliato, who gave helpful advice on the stability analysis involving a normal-cone feedback. The author would also like to thank the anonymous reviewers who shared their efforts to detect errors in equations in the draft version of this paper.

REFERENCES

[1] A. Peer and M. Buss, "A new admittance-type haptic interface for bimanual manipulations," *IEEE/ASME Trans. Mechatronics*, vol. 13, no. 4, pp. 416–428, Aug. 2008.

[2] R. Q. van der Linde and P. Lammertse, "HapticMaster—A generic force controlled robot for human interaction," *Ind. Robot*, vol. 30, no. 6, pp. 515–524, 2003.

[3] E. G. Kaigom and J. Roßmann, "Physics-based simulation for manual robot guidance—An eRobotics approach," *Robot. Comput.-Integr. Manuf.*, vol. 43, pp. 155–163, 2017.

[4] A. Campeau-Lecours, M. J.-D. Otis, and C. Gosselin, "Modeling of physical human-robot interaction: Admittance controllers applied to intelligent assist devices with large payload," *Int. J. Adv. Robot. Syst.*, vol. 13, no. 5, pp. 1–12, 2016.

[5] A. Morbi, M. Ahmadi, A. D. C. Chan, and R. Langlois, "Stability-guaranteed assist-as-needed controller for powered orthoses," *IEEE Trans. Control Syst. Technol.*, vol. 22, no. 2, pp. 745–752, Mar. 2014.

[6] A. Morbi and M. Ahmadi, "Safely rendering small impedances in admittance-controlled haptic devices," *IEEE/ASME Trans. Mechatronics*, vol. 21, no. 3, pp. 1272–1280, Jun. 2016.

[7] T. Osa, S. Uchida, N. Sugita, and M. Mitsuishi, "Hybrid rate-admittance control with force reflection for safe teleoperated surgery," *IEEE/ASME Trans. Mechatronics*, vol. 20, no. 5, pp. 2379–2390, Oct. 2015.

[8] R. Kikuuwe, "A sliding-mode-like position controller for admittance control with bounded actuator force," *IEEE/ASME Trans. Mechatronics*, vol. 19, no. 5, pp. 1489–1500, Oct. 2014.

[9] R. Kikuuwe, S. Yasukouchi, H. Fujimoto, and M. Yamamoto, "Proxy-based sliding mode control: A safer extension of PID position control," *IEEE Trans. Robot.*, vol. 26, no. 4, pp. 860–873, Aug. 2010.

[10] R. Kikuuwe and H. Fujimoto, "Proxy-based sliding mode control for accurate and safe position control," in *Proc. IEEE Int. Conf. Robot. Autom.*, 2006, pp. 25–30.

[11] V. Acary and B. Brogliato, *Numerical Methods for Nonsmooth Dynamical Systems: Applications in Mechanics and Electronics* (Lecture Notes in Applied and Computational Mechanics), vol. 35. New York, NY, USA: Springer, 2008.

[12] S. D. Eppinger and W. P. Seering, "On dynamic models of robot force control," *Proc. IEEE Int. Conf. Robot. Autom.*, 1986, vol. 3, pp. 29–34.

[13] S. D. Eppinger and W. P. Seering, "Three dynamic problems in robot force control," *IEEE Trans. Robot. Autom.*, vol. 8, no. 6, pp. 751–758, Dec. 1992.

[14] M. Dohring and W. S. Newman, "The passivity of natural admittance control implementations," in *Proc. IEEE Int. Conf. Robot. Autom.*, 2003, pp. 3710–3715.

[15] R. Kikuuwe, K. Kanaoka, T. Kumon, and M. Yamamoto, "Phase-lead stabilization of force-projecting master-slave systems with a new sliding mode filter," *IEEE Trans. Control Syst. Technol.*, vol. 23, no. 6, pp. 2182–2194, Nov. 2015.

[16] A. Calanca, R. Muradore, and P. Fiorini, "A review of algorithms for compliant control of stiff and fixed-compliance robots," *IEEE/ASME Trans. Mechatronics*, vol. 21, no. 2, pp. 613–624, Apr. 2016.

[17] A. Lecours and C. Gosselin, "Computed-torque control of a four-degree-of-freedom admittance controlled intelligent assist device," in *Experimental Robotics* (Springer Tracts in Advanced Robotics), vol. 88, J. Desai, G. Dudek, O. Khatib, and V. Kumar, Eds., New York, NY, USA: Springer, 2013, pp. 635–649.

[18] G. Peng, C. Yang, W. He, Z. Li, and D. Kuang, "Neural-learning enhanced admittance control of a robot manipulator with input saturation," in *Proc. Chin. Autom. Congr.*, 2017, pp. 104–109.

[19] O. Huber, V. Acary, B. Brogliato, and F. Plestan, "Implicit discrete-time twisting controller without numerical chattering: Analysis and experimental results," *Control Eng. Pract.*, vol. 46, pp. 129–141, 2016.

[20] B. Wang, B. Brogliato, V. Acary, A. Boubakir, and F. Plestan, "Experimental comparisons between implicit and explicit implementations of discrete-time sliding mode controllers: Toward input and output chattering suppression," *IEEE Trans. Control Syst. Technol.*, vol. 23, no. 5, pp. 2071–2075, Sep. 2015.

[21] V. Acary, B. Brogliato, and Y. Orlov, "Chattering-free digital sliding-mode control with state observer and disturbance rejection," *IEEE Trans. Autom. Control*, vol. 57, no. 5, pp. 1087–1101, May 2012.

[22] R. Kikuuwe, N. Takesue, A. Sano, H. Mochiyama, and H. Fujimoto, "Admittance and impedance representations of friction based on implicit Euler integration," *IEEE Trans. Robot.*, vol. 22, no. 6, pp. 1176–1188, Dec. 2006.

[23] H. K. Khalil, *Nonlinear Systems*, 3rd ed. Upper Saddle River, NJ, USA: Prentice-Hall, 2002.

[24] B. Brogliato, R. Lozano, B. Maschke, and O. Egeland, *Dissipative Systems Analysis and Control: Theory and Applications*, 2nd ed. New York, NY, USA: Springer, 2007.

[25] B. Brogliato and D. Goeleven, "Well-posedness, stability and invariance results for a class of multivalued Lur'e dynamical systems," *Nonlinear Anal.*, vol. 74, pp. 195–212, 2011.

[26] F. A. Miranda-Villatoro and F. Castaños, "Robust output regulation of strongly passive linear systems with multivalued maximally monotone controls," *IEEE Trans. Autom. Control*, vol. 62, no. 1, pp. 238–249, Jan. 2017.

[27] O. Huber, V. Acary, and B. Brogliato, "Lyapunov stability and performance analysis of the implicit discrete sliding mode control," *IEEE Trans. Autom. Control*, vol. 61, no. 10, pp. 3016–3030, Oct. 2016.

[28] F. A. Miranda-Villatoro, F. Castaños, and B. Brogliato, "A set-valued nested sliding-mode controller," *IFAC PapersOnLine*, vol. 50, no. 1, pp. 2971–2976, 2017.

[29] M. T. S. Aung, R. Kikuuwe, and M. Yamamoto, "Friction compensation of geared actuators with high presliding stiffness," *J. Dyn. Syst., Meas., Control*, vol. 137, no. 1, 2015, Art. no. 011007.

[30] M. Iwatani and R. Kikuuwe, "Some improvements in elastoplastic friction compensator," *SICE J. Control, Meas., Syst. Integr.*, vol. 10, no. 3, pp. 141–148, 2017.

[31] M. T. S. Aung and R. Kikuuwe, "Stability enhancement of admittance control with acceleration feedback and friction compensation," *Mechatronics*, vol. 45, pp. 110–119, 2017.

[32] M. Iwatani and R. Kikuuwe, "An elastoplastic friction force estimator and its application to external force estimation and force-sensorless admittance control," in *Proc. IEEE/SICE Int. Symp. Syst. Integr.*, 2016, pp. 45–50.

[33] B. Yao, Z. Zhou, L. Wang, W. Xu, Q. Liu, and A. Liu, "Sensorless and adaptive admittance control of industrial robot in physical human-robot interaction," *Robot. Comput.-Integr. Manuf.*, vol. 51, pp. 158–168, 2018.

[34] F. Facchinei and J.-S. Pang, *Finite-Dimensional Variational Inequalities and Complementarity Problems, Volume I*. New York, NY, USA: Springer, 2003.

[35] A. Fischer, "A special Newton-type optimization method," *Optimization*, vol. 24, no. 3/4, pp. 269–284, 1992.

[36] C. Kanzow, "Some noninterior continuation methods for linear complementarity problems," *SIAM J. Matrix Anal. Appl.*, vol. 17, no. 4, pp. 851–868, 1996.

[37] M. Fukushima, Z.-Q. Luo, and P. Tseng, "Smoothing functions for second-order-cone complementarity problems," *SIAM J. Optim.*, vol. 12, no. 2, pp. 436–460, 2002.

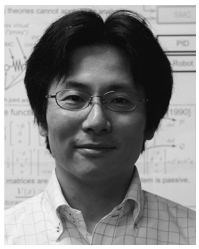

Ryo Kikuuwe (S'02–M'03) received the B.S., M.S. and Ph.D. (Eng.) degrees in mechanical engineering from Kyoto University, Kyoto, Japan, in 1998, 2000, and 2003, respectively.

From 2003 to 2007, he was an Endowed-Chair Research Associate with the Nagoya Institute of Technology, Nagoya, Japan. From 2007 to 2017, he was an Associate Professor with the Department of Mechanical Engineering, Kyushu University, Fukuoka, Japan. From 2014 to 2015, he was a Visiting Researcher with Institut National de Recherche en Informatique et en Automatique (INRIA) Grenoble Rhône-Alpes, Saint Ismier, France. He is currently a Full Professor with the Department of Mechanical Systems Engineering, Hiroshima University, Higashi-Hiroshima, Japan. His research interests include force control of robot manipulators, real-time simulation for physics-based animation, and engineering applications of differential inclusions.

Prof. Kikuuwe is a member of the Robotics Society of Japan, the Japan Society of Mechanical Engineers, the Society of Instrument and Control Engineers (Japan), and the Virtual Reality Society of Japan. He was a recipient of the Best Paper Award of Advanced Robotics in 2013 and the Young Investigator Excellence Award from the Robotics Society of Japan in 2005.